Natural killer T cells in adipose tissue prevent insulin resistance

Henk S. Schipper,[1,2,3] Maryam Rakhshandehroo,[1] Stan F.J. van de Graaf,[1,3] Koen Venken,[4] Arjen Koppen,[1,3] Rinke Stienstra,[5,6] Serge Prop,[1] Jenny Meerding,[2] Nicole Hamers,[1,3] Gurdyal Besra,[7] Louis Boon,[8] Edward E.S. Nieuwenhuis,[2] Dirk Elewaut,[4] Berent Prakken,[2] Sander Kersten,[5] Marianne Boes,[2] and Eric Kalkhoven[1,2,3]

[1]Department of Metabolic Diseases, University Medical Center Utrecht, Utrecht, the Netherlands. [2]Department of Pediatric Immunology and Infectious Diseases, University Medical Center Utrecht and Center for Molecular and Cellular Intervention, University Medical Center Utrecht, Wilhelmina Children's Hospital, Utrecht, the Netherlands. [3]Netherlands Metabolomics Center, Leiden, the Netherlands. [4]Department of Rheumatology, Faculty of Medicine and Health Sciences, Laboratory for Molecular Immunology and Inflammation, Ghent University, Ghent, Belgium. [5]Nutrition, Metabolism, and Genomics Group, Division of Human Nutrition, Wageningen University, Wageningen, the Netherlands. [6]Department of Medicine, Radboud University Nijmegen Medical Centre, Nijmegen, the Netherlands. [7]School of Biosciences, University of Birmingham, Edgbaston, Birmingham, United Kingdom. [8]Bioceros BV, Utrecht, the Netherlands.

Lipid overload and adipocyte dysfunction are key to the development of insulin resistance and can be induced by a high-fat diet. CD1d-restricted invariant natural killer T (iNKT) cells have been proposed as mediators between lipid overload and insulin resistance, but recent studies found decreased iNKT cell numbers and marginal effects of iNKT cell depletion on insulin resistance under high-fat diet conditions. Here, we focused on the role of iNKT cells under normal conditions. We showed that iNKT cell–deficient mice on a low-fat diet, considered a normal diet for mice, displayed a distinctive insulin resistance phenotype without overt adipose tissue inflammation. Insulin resistance was characterized by adipocyte dysfunction, including adipocyte hypertrophy, increased leptin, and decreased adiponectin levels. The lack of liver abnormalities in CD1d-null mice together with the enrichment of CD1d-restricted iNKT cells in both mouse and human adipose tissue indicated a specific role for adipose tissue–resident iNKT cells in the development of insulin resistance. Strikingly, iNKT cell function was directly modulated by adipocytes, which acted as lipid antigen-presenting cells in a CD1d-mediated fashion. Based on these findings, we propose that, especially under low-fat diet conditions, adipose tissue–resident iNKT cells maintain healthy adipose tissue through direct interplay with adipocytes and prevent insulin resistance.

Introduction

More than one-third of the U.S. population has insulin resistance, a condition that is predominantly caused by obesity and is associated with adipocyte dysfunction together with chronic low-grade adipose tissue (AT) inflammation (1–3). Lipid-induced adipocyte dysfunction appears instrumental to the inflammatory response in AT (4), which is characterized by inflammasome activation (5) and the release of fatty acids and cytokines (adipokines) that impair insulin receptor signaling, ultimately resulting in the development of metabolic syndrome (6–8).

Distinct mechanisms impart control of immune homeostasis within AT, some of which were recently uncovered. AT-resident Tregs together with eosinophils control the development of local inflammation by counteracting the influx of $CD11c^+$ (M1) inflammatory macrophages, $CD8^+$ T cells, $CD4^+$ T cells, and B cells, thereby preventing AT inflammation and insulin resistance (9–16). How adipocyte dysfunction relates to immune homeostasis, however, remains incompletely understood, and a self-reactive cell type involved in orchestrating immune homeostasis in AT has not yet been reported.

Various findings prompted us to study the role of lipid antigen–reactive invariant natural killer T cells (iNKT) cells in controlling AT inflammation and insulin resistance. First, the abundance of lipid antigens in AT preeminently suits lipid-sensitive invariant T cells such as iNKT cells, as they are triggered to release immune-polarizing cytokines by lipid/CD1d complex binding (17–19). Second, CD1d-restricted iNKT cells have roles in multiple metabolic disease models, including type 1 diabetes mellitus (20–23). Third, many tissues harbor resident T cells that can respond to stress-induced self molecules rather than foreign antigens and ensure a tissue-specific effector class (Th1, Th2, or tolerogenic) response (24). iNKT cells are known to fulfill this role in the liver, representing up to 40% of liver-resident T cells in mice (19). Fourth, we were intrigued by the apparent enrichment of iNKT cells in mouse and human AT compared with peripheral blood (our unpublished observations and refs. 25, 26), especially in lean mice and humans. Fifth, recent studies showed that under high-fat diet (HFD) conditions, CD1d-restricted iNKT cell function only marginally affects the development of insulin resistance (26–28). Accordingly, we hypothesized that AT-resident CD1d-restricted iNKT cell function may be particularly relevant under normal diet conditions.

We employed CD1d-null and Jα18-null mice, antibody depletion of iNKT cells in WT mice, and human AT to address the role of AT-resident CD1d-restricted iNKT cells. Our mouse-based data show a unique role for CD1d-restricted iNKT cells in the maintenance of healthy adipocytes and prevention of insulin resistance, especially under low-fat diet (LFD) conditions, considered a normal diet for mice (29). Furthermore, coculture of human CD1d-restricted iNKT cells with adipocytes revealed a potential mechanism linking adipocyte dysfunction to immune

Authorship note: Marianne Boes and Eric Kalkhoven contributed equally to this work.
Conflict of interest: The authors have declared that no conflict of interest exists.
Citation for this article: *J Clin Invest.* 2012;122(9):3343–3354. doi:10.1172/JCI62739.

cell homeostasis, showing that CD1d-proficient adipocytes can function as lipid APCs for iNKT cells.

Results

iNKT cell knockout and antibody-mediated depletion result in insulin resistance in lean mice. We addressed the impact of CD1d-restricted iNKT cells on AT homeostasis and insulin resistance using CD1d-null (30) and WT C57BL/6 mice. The mice were fed normal chow until 11 weeks of age, followed by 19 weeks of LFD or HFD. Weight gain, caloric intake, and epididymal fat pad weight were similar among the genotypes, for both LFD and HFD mouse groups (Figure 1, A–C). Strikingly, glucose tolerance measured via an intraperitoneal glucose tolerance test (IP-GTT) was clearly impaired in the CD1d-null mice compared with their WT counterparts, especially under LFD conditions (Figure 1, D–G). Under HFD conditions, CD1d-null mice showed higher insulin levels during the IP-GTT than their WT counterparts, but maintained comparable glucose levels (Figure 1, D–G), in accordance with previous studies (26–28). To corroborate these findings, we used of Jα18-null mice, which are selectively deficient in type 1 iNKT cells (31). These animals also showed impaired glucose tolerance after 18 weeks of LFD compared with their WT counterparts (Figure 1, H and I) while maintaining comparable body weight (data not shown).

The insulin resistance in lean CD1d-null and Jα18-null mice was confirmed using an established iNKT depletion model, comparing antibody-treated (anti-NK1.1) with isotype control–treated LFD-fed WT mice (32, 33). Partial depletion of AT-resident iNKT cells resulted in impaired glucose tolerance compared with isotype control treatment (Figure 1, J and K, and Supplemental Figure 1A; supplemental material available online with this article; doi:10.1172/JCI62739DS1). When a gain-of-function approach was pursued by in vivo activation of iNKT cells in WT mice on LFD through injection of the CD1d-restricted iNKT cell ligand α-galactosyl ceramide (αGalCer), glucose tolerance did not improve (Supplemental Figure 2C and ref. 26), probably due to the fact that WT animals are highly insulin sensitive under LFD conditions. Taken together, these findings indicate that CD1d-restricted iNKT cells protect against insulin resistance, especially in LFD-fed mice.

As iNKT cells reside not only in AT (Figure 2) but also in the liver, and both organs are critically involved in the regulation of whole-body lipid and glucose homeostasis (34), we investigated circulating lipids and liver function in CD1d-null mice, focusing on LFD conditions. While circulating triglycerides were slightly elevated in CD1d-null mice on a LFD, circulating FFA and cholesterol levels were not (Supplemental Figure 1, B–D). More importantly, CD1d-null mice on a LFD showed none of the pathological alterations that are associated with liver-mediated insulin resistance (35): neither liver histology, weight, and lipid content nor the liver enzymes aspartate aminotransferase (AST) and alanine aminotransferase (ALT) and the liver inflammatory markers lipocalin-2 (*Lcn2*) and serum amyloid A (*Saa2*) were altered in CD1d-null mice on a LFD, compared with their WT counterparts (Supplemental Figure 1, E–K). In WT and CD1d-null mice under HFD conditions, though, liver pathology was observed; for some parameters, this was most pronounced in CD1d-null mice (Supplemental Figure 1, E–K). These findings argue against a principal role for the liver in the insulin-resistant phenotype observed in LFD-fed CD1d-null and iNKT cell–depleted mice. We therefore focused on the role of AT-resident iNKT cells.

AT-resident iNKT cells show an antiinflammatory phenotype and are downregulated on a long-term HFD. AT-resident iNKT cells constitute 5%–10% of the visceral AT–resident (VAT-resident) T lymphocyte pool, as indicated by αGC-loaded CD1d tetramer and TCRβ staining (Figure 2A). Compared with spleen-derived iNKT cells, which are predominantly $CD4^+$ and clearly express NK1.1, AT-resident iNKT cells exhibit a phenotype biased toward CD4/CD8 double-negative (~70%) with reduced NK1.1 expression (~50%) (Figure 2, A, D, and E). Next, AT-resident iNKT cell cytokine production was analyzed. AT-resident iNKT cells showed an antiinflammatory phenotype with high levels of intracellular IL-4 and IL-13 and lower levels of IFN-γ compared with splenic iNKT cells (Figure 2B). Production of all 3 cytokines was increased upon in vivo treatment with αGalCer, both in AT and splenic iNKT cells (Figure 2B). Functionality of AT-resident iNKT cells (i.e., cytokine production) was confirmed by ex vivo stimulation experiments (Supplemental Figure 2B). To address the contribution of iNKT cells to cytokine production in AT, we performed quantitative RT-PCR analysis on AT from WT and CD1d-null mice. A decrease in *Il4* and *Il13* mRNA levels in particular was observed in CD1d-null mice, indicating that iNKT cells contribute to the presence of these cytokines in AT (Figure 2C). We noticed a decrease in iNKT numbers in VAT and in subcutaneous AT (SCAT) in WT mice fed a HFD compared with a LFD (Figure 2F), which was not due to TCRβ downregulation (data not shown). In addition, reduced expression of signaling lymphocytic activation molecule f1 (SLAMf1) (36, 37) on the remaining iNKT cells was observed (Supplemental Figure 2A). Thus, low iNKT cell numbers and activity under HFD conditions may partly explain the relatively small differences in glucose tolerance observed between WT and CD1d-null mice on a long-term HFD.

CD1d-null mice exhibit enhanced AT Treg numbers, preventing worsening of insulin resistance. We next asked whether iNKT cells prevent the insulin resistance in CD1d-null mice on a LFD through an immune-modulatory mechanism, as shown in other tissues (17–19). Under HFD conditions, AT infiltration of $CD8^+$ T cells, followed by infiltration of macrophages that exhibit an M1-polarized phenotype, plays a pivotal role in the development of insulin resistance (13, 38). However, CD1d-null mice on a LFD exhibited neither AT $CD8^+$ T cell infiltration nor increased macrophage numbers and M1 polarization (Figure 3, A and B, and Supplemental Figure 3A). Only under HFD conditions did we observe increased macrophage numbers and M1 polarization in CD1d-null mice compared with their WT counterparts (Supplemental Figure 3, A and B). Instead, higher $CD4^+CD25^+$ T cell numbers were detected in AT of CD1d-null mice, on both LFD and HFD (Figure 3C and Supplemental Figure 3B). $CD4^+CD25^+$ T cells extracted from AT expressed high levels of Foxp3 (Figure 3D), and the number of $CD4^+Foxp3^+$ T cells (but not their MFI) was increased in the iNKT cell–depleted mice (Figure 3E and data not shown). Thus, complete absence of iNKT cells in CD1d-null mice and antibody-mediated iNKT cell depletion both result in an enrichment of Tregs in AT. Considering the protective role of Tregs in AT (9), we next addressed whether the increased Treg numbers prevent worsening of the insulin resistance phenotype. Upon anti-CD25 antibody–mediated depletion of Tregs in the CD1d-null mice on a LFD, an aggravation of the insulin-resistant phenotype observed in CD1d-null mice was seen (Figure 3, F and G, and Supplemental Figure 3C). Pointing to the importance of iNKT cells for this effect, depletion

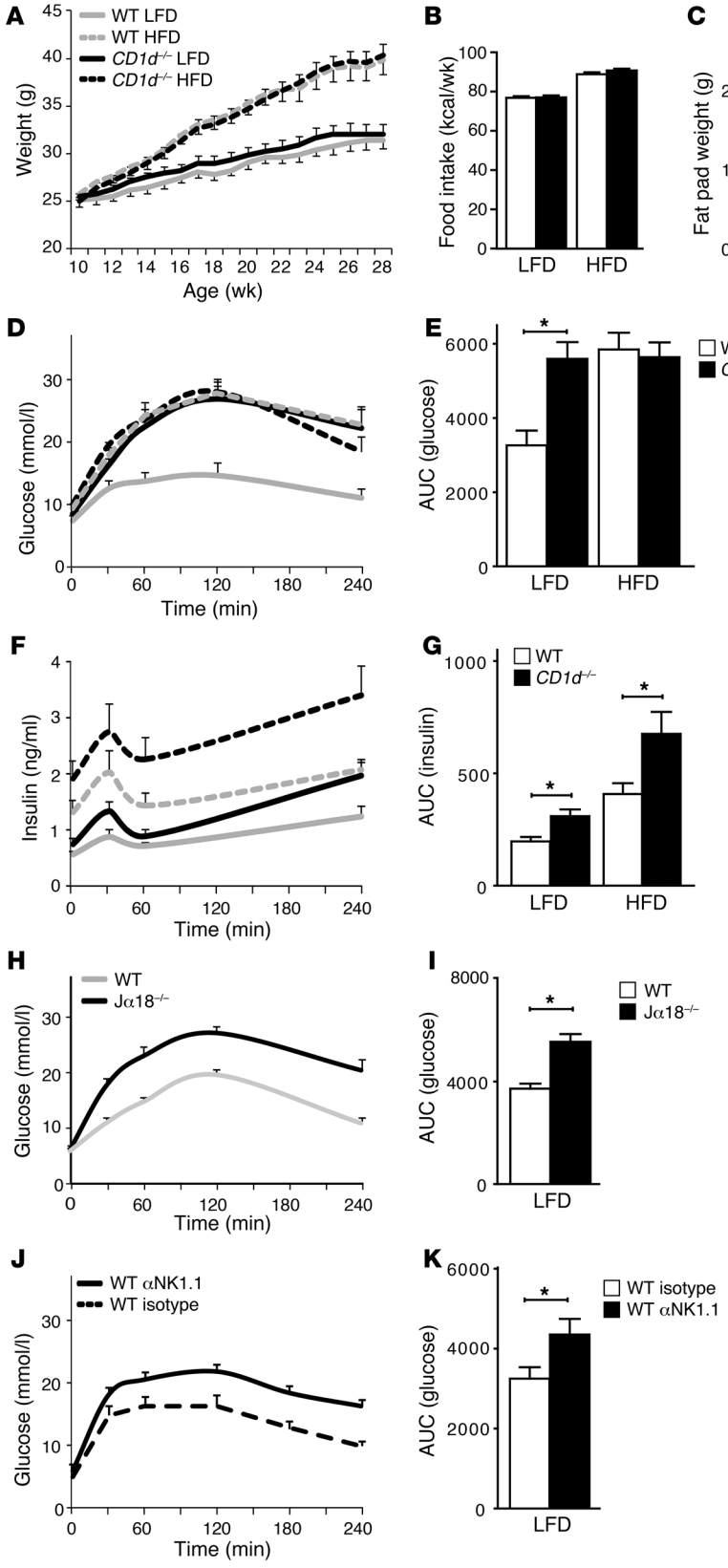

Figure 1

iNKT cell knockout and antibody-mediated depletion result in insulin resistance in lean mice. For **A**–**H**, n = 10 mice per group; total 40 mice. (**A**) Weight gain of WT and CD1d-null mice on the LFD and HFD regimens. Mice were weighed weekly. (**B**) Weekly caloric intake of WT and CD1d-null mice on the LFD and HFD regimens. (**C**) Epididymal fat pad weights of the WT and CD1d-null mice on a LFD and HFD regimen, measured after termination. (**D** and **E**) IP-GTTs were performed after 17 weeks of LFD or HFD. Plasma glucose concentrations and the AUC for the various groups are shown. (**F** and **G**) Plasma insulin levels during the IP-GTT are shown, together with the AUC. (**H** and **I**) IP-GTT of WT and Jα18-null mice after 18 weeks of LFD. Shown are plasma glucose concentrations and the AUC for the 2 groups. n = 15 mice per group; total 30 mice. (**J** and **K**) IP-GTT of WT (Isotype) and iNKT cell–depleted (αNK1.1) WT mice. Note that this antibody also depletes NK cells. Shown are plasma glucose concentrations and the AUC for the 2 groups. n = 10 mice per group; total 20 mice. $^*P < 0.05$.

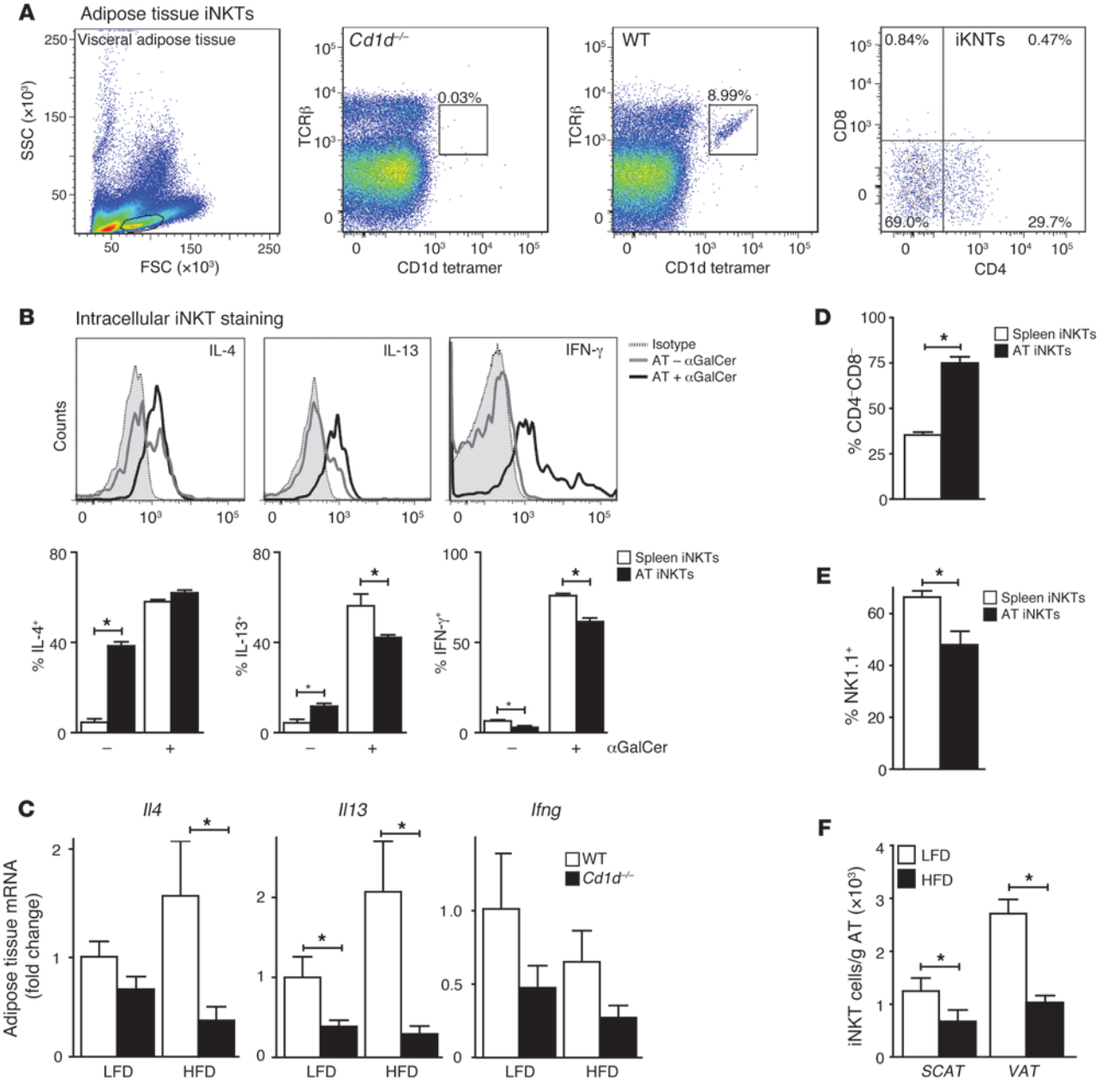

Figure 2

AT-resident iNKT cells show an activated phenotype and are downregulated on a long-term HFD. (**A**) Stromal vascular fraction of visceral adipose tissue (VAT) from WT and CD1d-null mice was stained for TCRβ, CD1d tetramer, CD4, and CD8. FSC, forward scatter; SSC, side scatter. Numbers in graphs indicate the percentage of cells in that gate. Second and third panel, percentage of TCRβ$^+$ cells; fourth panel, CD4 and CD8 staining of iNKT cells. (**B**) Intracellular staining of spleen and visceral AT-extracted iNKT cells from 4 WT mice, injected intraperitoneally with αGalCer (5 μg) or vehicle. Shown are representative histograms and averages in bar graphs. (**C**) Quantitative RT-PCR on VAT of WT and CD1d-null mice on the LFD and HFD regimens. n = 9 mice per group; total 36 mice. (**D** and **E**) Percentage of CD4$^-$CD8$^-$ and NK1.1$^+$ iNKT cells (gated on TCRβ and CD1d/αGC-loaded tetramer) extracted from spleen and VAT of WT mice on a LFD. n = 10 mice per group; total 20 mice. (**F**) Number of iNKT cells per gram of SCAT and VAT of WT mice on LFD and HFD regimens. n = 10 mice per group; total 20 mice. *P < 0.05.

of Tregs in the WT mice on a LFD had no effect (Supplemental Figure 3D). Taken together, the results indicated that CD1d-null mice on a LFD have a unique AT phenotype that, unlike the well-studied HFD phenotype, is characterized not by increased influx of proinflammatory CD8$^+$ T cell or macrophage populations, but rather by increased Treg numbers. The increase in AT Tregs observed upon iNKT cell depletion may serve to prevent further aggravation of insulin resistance.

Absence of CD1d-restricted iNKT cells is associated with adipocyte dysfunction in lean mice. Using an Affymetrix microarray platform, we explored further the AT phenotype in CD1d-null mice on a LFD. Microarray analysis underscored that the AT phenotype

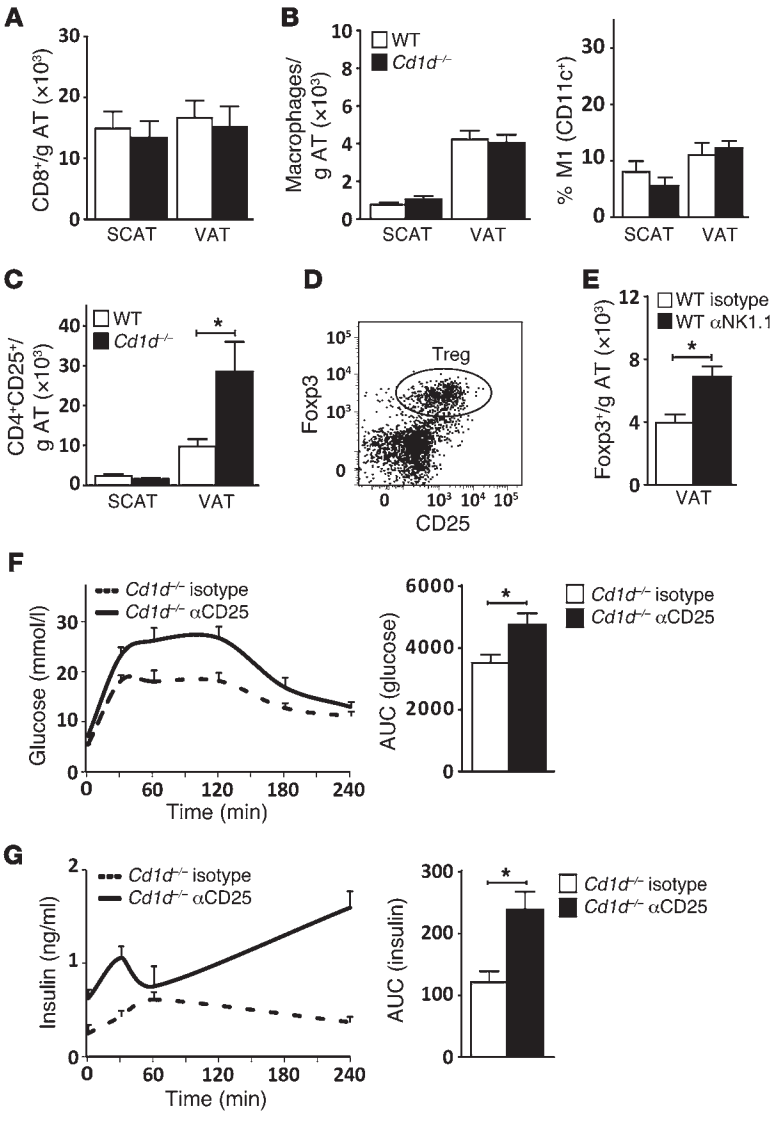

Figure 3

CD1d-null mice exhibit enhanced AT Treg numbers, preventing worsening of insulin resistance. (**A**–**C**) n = 10 mice per group; total 20 mice. (**A**) Number of CD8$^+$ T cells (TCRβ$^+$) per gram of SCAT and VAT, for WT and *Cd1d*$^{-/-}$ mice on a LFD. (**B**) Number of macrophages (F4/80$^+$) per gram of SCAT and VAT, and percentage of M1-polarized (CD11c$^+$) macrophages for WT and *Cd1d*$^{-/-}$ mice on a LFD. (**C**) Number of CD4$^+$CD25$^+$ T cells (TCRβ$^+$) per gram of SCAT and VAT for WT and *Cd1d*$^{-/-}$ mice on a LFD. (**D**) Representative results of staining of Foxp3 and CD25 expression on AT-derived CD4$^+$ T cells (TCRβ$^+$) in *Cd1d*$^{-/-}$ mice. (**E**) Number of Tregs (TCRβ$^+$CD4$^+$Foxp3$^+$) per gram of VAT for WT (Isotype) and iNKT cell–depleted (αNK1.1) WT mice. n = 10 mice per group; total 20 mice. (**F** and **G**) IP-GTT of *Cd1d*$^{-/-}$ (Isotype) and Treg-depleted (αCD25) CD1d-null mice on a LFD. Shown are plasma glucose and insulin concentrations, together with the AUC for the 2 groups. n = 10 mice per group; total 20 mice. *$P < 0.05$.

in lean insulin-resistant CD1d-null mice is different from the HFD-associated disease pattern. Classical inflammatory markers upregulated under HFD conditions, including *Tnfa*, Emr1 hormone receptor (*F4/80*), integrin alpha X (*Cd11c*), *Ccl2*, serum amyloid a 3 (*Saa3*), and a disintegrin and metallopeptidase domain 8 (*Adam8*) (39–41) were not different in LFD-fed CD1d-null mice and their WT counterparts (Figure 4, A and B). The effect of long-term HFD on the transcriptional profile was remarkably similar in both genotypes (Supplemental Figure 4), in accordance with the reduced AT-resident iNKT numbers detected under long-term HFD conditions (Figure 2F). Next, we focused on adipocyte function in LFD-fed CD1d-null mice. Along with inflammatory changes, adipocyte dysfunction, characterized by adipocyte hypertrophy and altered adipokine secretion (1), is key to the development of insulin resistance. Indeed, enlarged adipocytes (larger area per adipocyte and lower number of adipocytes per field) were found in the CD1d-null mice on a LFD compared with their WT counterparts (Figure 4C and Supplemental Figure 4C), but there was no difference in epididymal fat pad weight (Figure 1C) or total fat mass as determined by dual energy X-ray absorptiometry (DEXA) scanning (Supplemental Figure 4D). No changes in several genes involved in lipogenesis (stearoyl-coenzyme A desaturase 1, *Scd1*; fatty acid synthase, *Fas*), lipid droplet formation (perilipin 1, *Lipin1*, *Pparg*), and thermogenesis (uncoupling protein 1, *Ucp1*; *Ppara*) were detected in LFD-fed CD1d-null mice, except for a significant increase in lipin (Supplemental Figure 4E), an adiposity gene involved in triglyceride synthesis (42). Lipolysis, as determined by plasma glycerol levels, was also not significantly changed (Supplemental Figure 4F). Remarkably, the adipocyte dysfunction in LFD-fed CD1d-null mice was reflected by decreased levels of the insulin-sensitizing adipokine adiponectin and increased levels of the insulin-desensitizing leptin (43), at both the mRNA level in the AT and the protein level in the plasma (Figure 4, D and E). Thus, development of insulin resistance in the absence of iNKT cells may originate from adipocyte dysfunction, in particular altered adipokine secretion.

Enrichment of CCR2$^+$ iNKT cells in human AT. Having investigated mouse AT-resident iNKT cells, we set out to study the role of iNKT cells in human AT. We first assessed the relative number of iNKT cells as a fraction of lymphocytes in paired blood and abdominal SCAT samples obtained from healthy donors (n = 6). iNKT cell numbers were enriched approximately 10-fold in AT compared with blood (flow cytometry analyses, using TCR Vα24/Vβ11 and CD3/αGC-loaded CD1d tetramer staining) (Figure 5, A and B). In AT and blood, 30% of the iNKT population consisted of CD4$^+$ iNKT cells, with the remaining fraction mostly representing CD4$^-$CD8$^-$ iNKT cells (Figure 5, A and C). We considered the possibility that iNKT cells are recruited to AT. To this end, we determined the expression of a range of chemokine receptors on iNKT cells purified from blood and AT, including CCR2, CCR4, CCR5, CCR7, CXCR2, CXCR3, CXCR6, and CX3CR1, as well as CD62L and CD11b (44). Significantly increased expression levels on iNKT cells from AT compared with blood were observed for CCR2, the chemokine receptor for the AT-secreted MCP-1 (45), and for the chemokine receptors CXCR2 and CXCR6, while expression levels of the other chemo-

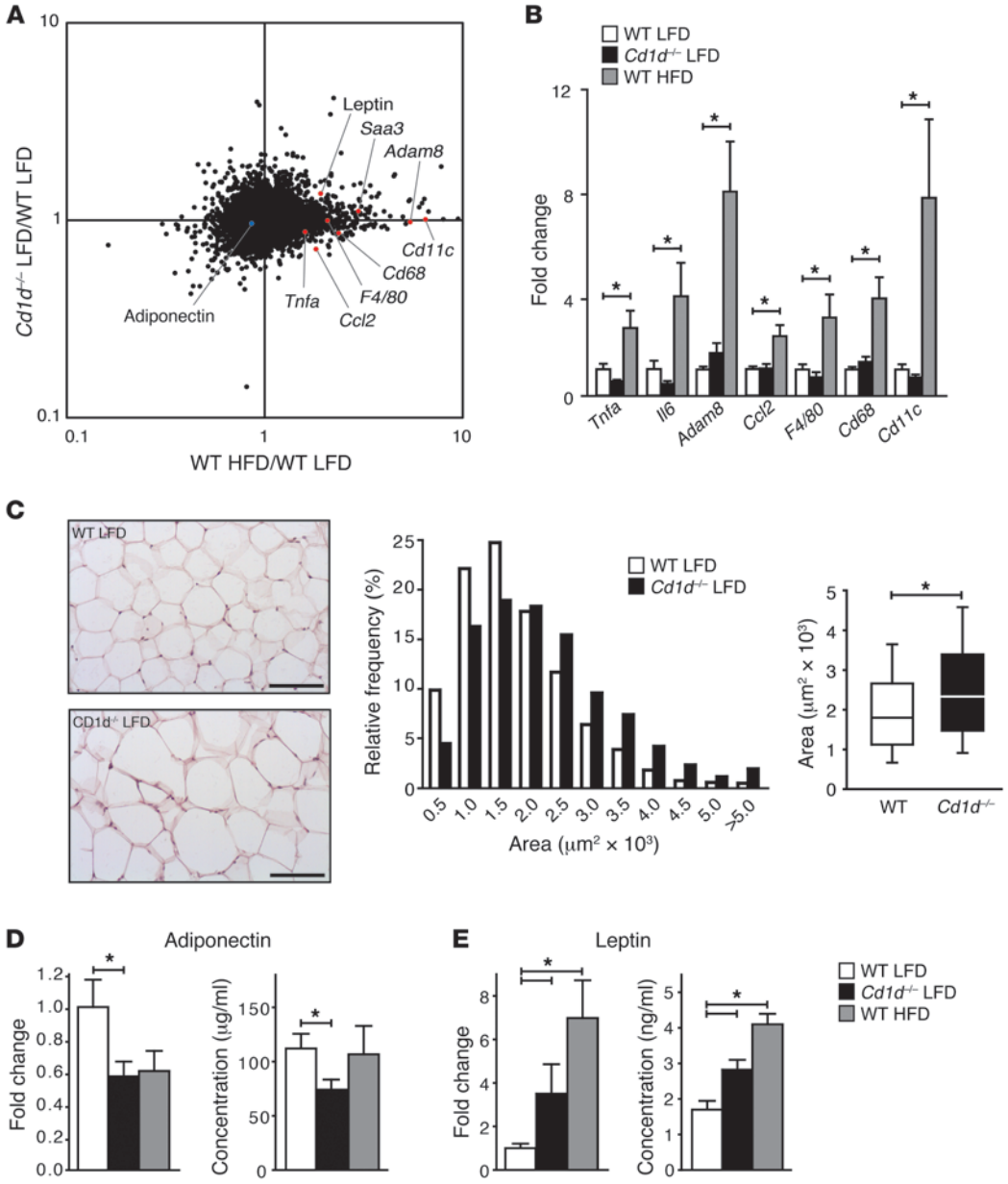

Figure 4

Absence of CD1d-restricted iNKT cells is associated with adipocyte dysfunction in lean mice. (**A**) Microarray-based fold change versus fold change scatter plot comparing gene expression profiles in WT HFD group (*x* axis) and *Cd1d*$^{-/-}$ LFD group (*y* axis). Genes of interest encoding classical inflammatory markers or adipokines are highlighted in red (upregulated) or blue (downregulated). Fold changes represent the mean of 4–6 mice per experimental group. (**B**) Quantitative RT-PCR of selected classical inflammatory markers in AT. Mean expression in WT LFD mice was set at 1. Fold changes were normalized for housekeeping gene expression (*36B4*). *n* = 9 mice per group; total 27 mice. (**C**) H&E staining of VAT from WT and CD1d-null mice after 19 weeks of LFD feeding. Scale bars: 100 μm. VAT adipocyte sizes (area per adipocyte, μm^2) in LFD-fed WT and CD1d-null mice are presented. Box plots show the median area per adipocyte for both groups, and 10th to 90th percentiles. *n* = 10 mice per group; total 20 mice. (**D** and **E**) Leptin and adiponectin mRNA expression in VAT were determined by quantitative RT-PCR (*n* = 9 mice per group; total 27 mice). Leptin and adiponectin protein levels were analyzed in plasma from LFD-fed CD1d-null mice and WT mice on a LFD and HFD. *n* = 10 mice per group; total 30 mice.

kine receptors and CD62L and CD11b were similar in iNKT cells from AT and blood (Figure 5D and Supplemental Figure 5A). Thus, MCP-1/CCR2–mediated and CXCR2- and CXCR6-mediated chemotaxis may provide a mechanism for the recruitment of iNKT cells to AT.

Human adipocytes express Cd1d and can regulate iNKT cell function. Adipocytes are a major constituent of AT and contain lipids that may serve as CD1d antigenic ligands. Therefore, we tested the possibility that adipocytes directly modulate iNKT cell function by presenting lipid antigens. First, the expression of CD1d and its

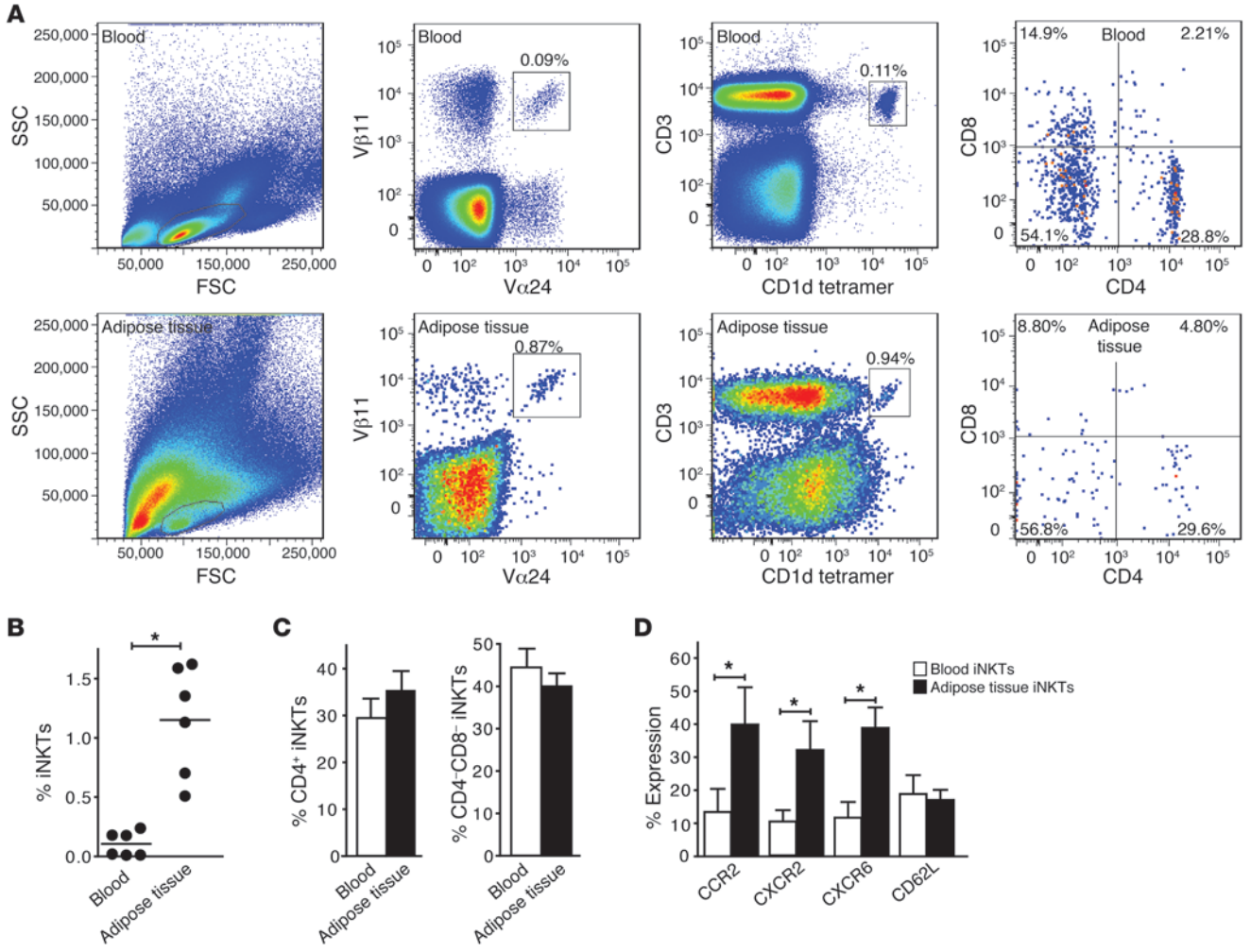

Figure 5

Enrichment of CCR2+ iNKT cells in human AT. (**A**) Blood and AT-derived iNKT cells were stained for Vα24, Vβ11, CD1d tetramer, and CD4 and CD8 expression. iNKT cell percentages of the total CD3+ population are shown. For **B**–**D**, $n = 6$ healthy donors. (**B** and **C**) iNKT cell contribution to the total CD3+ T cell population in blood and AT, and the percentage of CD4+ and CD4/CD8 double negative iNKT cells. (**D**) Chemokine receptor and CD62L expression on blood and AT-derived iNKT cells (gated on CD3 and CD1d/αGC-loaded tetramer). *$P < 0.05$.

lipid-loading machinery was analyzed in human SGBS (pre)adipocytes, a well-established adipocyte cell culture model (46), and in human primary adipocytes by quantitative RT-PCR. Several known components required for antigen loading (pro-saposin, *NPC2*, α-galactisodase) as well as *CD1D* itself were expressed at background levels in undifferentiated preadipocytes, but were readily detectable in mature human SGBS adipocytes and primary adipocytes (Figure 6A). Of note, CD1d depletion by lentivirally transduced CD1d shRNA in human preadipocytes did not influence their differentiation potential, adipocyte marker expression, or adiponectin secretion, suggesting that CD1d expression is not essential for differentiation and function of cultured (pre) adipocytes (Supplemental Figure 5, B and C). The upregulation of CD1d and its loading machinery as measured by increased mRNA gene transcription in mature human adipocytes suggests that adipocytes can function as lipid APCs for iNKT cells. To test this possibility, we generated short-term iNKT cell lines (>70% CD1d-restricted iNKT cells) from 5 healthy blood donors (47) and cocultured them with human adipocyte cell lines, where indicated displaying reduced CD1d expression upon shRNA-mediated knockdown or overexpressing CD1d (Supplemental Figure 5B and Supplemental Figure 6A). After loading of mature adipocytes with αGalCer (48) and 18 hours of coculture, the production of IL-4, IL-13, and IFN-γ by the iNKT cells was assessed. Strikingly, iNKT cells cocultured with mature adipocytes showed the highest intracellular IL-4, IL-13, and IFN-γ levels. The intracellular cytokine levels were found to be reduced upon CD1d blocking and depleted to background levels by CD1d knockdown (Figure 6B and Supplemental Figure 6B). Interestingly, basal cytokine levels were also decreased by CD1d knockdown, suggesting that adipocytes can present lipid autoantigens (Figure 6B and Supplemental Figure 6B). Cytokine measurements in the supernatant were affirmative, again showing only IL-4, IL-13, and IFN-γ release for iNKT cells cocultured with mature adipocytes. Also here cytokine release was reduced upon CD1d blocking and fully depleted by CD1d knockdown (Figure 6C and Supplemental Fig-

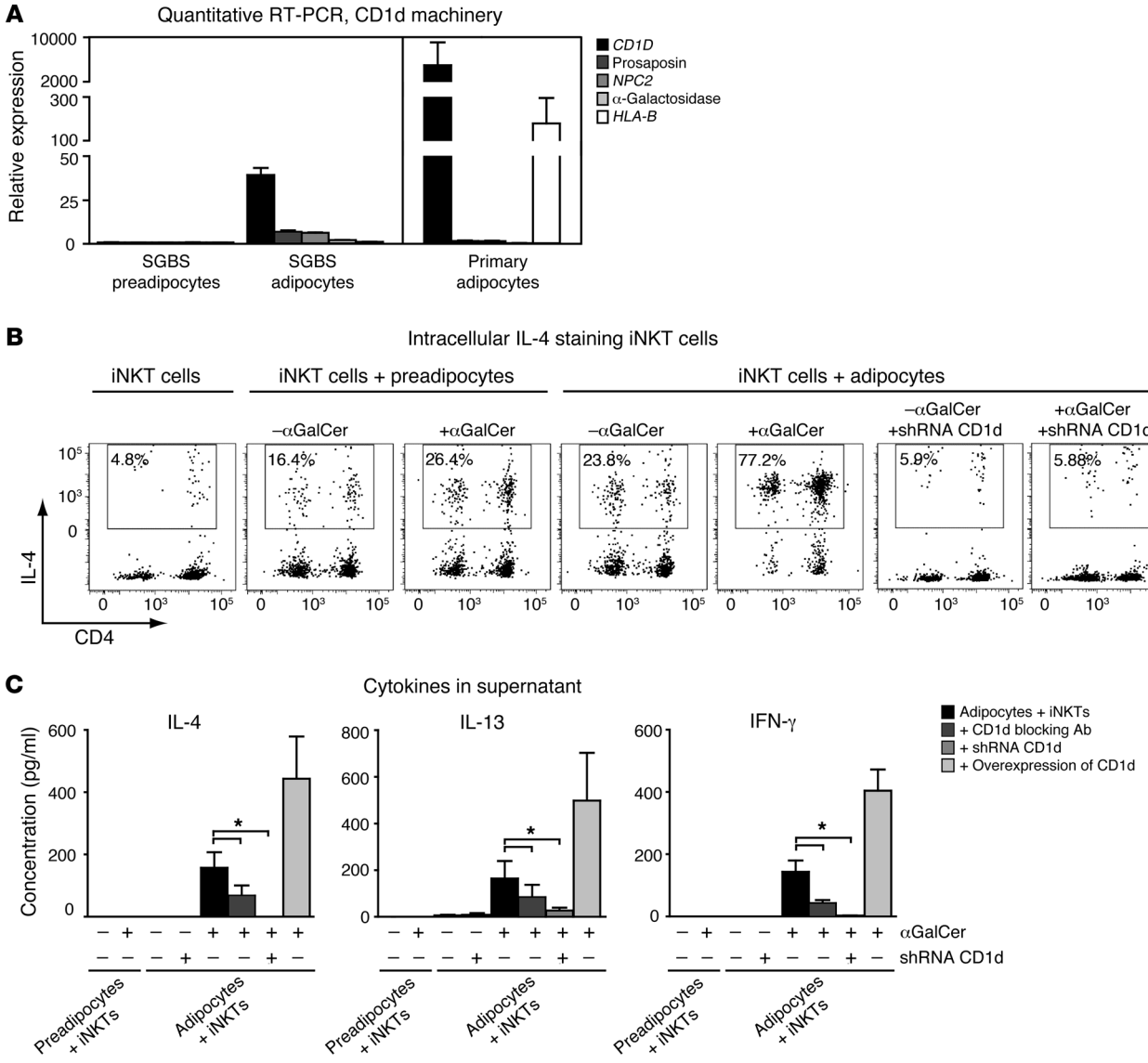

Figure 6

Adipocytes can modulate iNKT cell function in a CD1d-dependent manner. (**A**) Quantitative RT-PCRs of *CD1d* and its lipid-loading machinery genes pro-saposin, *NPC2*, and α-galactosidase in human SGBS preadipocytes, mature adipocytes, and primary subcutaneous adipocytes isolated from 3 human subjects. *HLA-B* mRNA levels were included as a negative control. Fold changes were normalized for housekeeping genes (*36B4* and β2 actin). (**B**) Intracellular IL-4 staining of iNKT cells cocultured with undifferentiated SGBS preadipocytes and mature adipocytes, with and without prior loading of the (pre)adipocytes with the CD1d-restricted iNKT cell ligand αGalCer. CD1d knockdown in the adipocytes depleted intracellular IL-4 staining in the cocultured iNKT cells. (**C**) IL-4, IL-13, and IFN-γ levels in the supernatants of iNKT cells cocultured with undifferentiated SGBS preadipocytes and mature adipocytes. Antibody blocking and CD1d knockdown of CD1d in mature adipocytes result in a significant decrease in IL-4, IL-13, and IFN-γ levels in the supernatants, while CD1d overexpression results in an increase. Data represent the mean results of 5 different iNKT cell lines cocultured with the (pre)adipocytes. $^*P < 0.05$.

ure 6C). Taken together, our results show that mature human adipocytes express functional CD1d and can act as lipid APCs, modulating iNKT cell function.

Discussion

In recent years, various AT-resident immune cells have been implicated in the regulation of lipid and glucose homeostasis (9, 13, 14). Here we show that AT-resident CD1d-restricted iNKT cells protect against the development of insulin resistance by preventing adipocyte dysfunction, especially under LFD conditions. The high numbers of CD1d-restricted iNKT cells in both mouse and human AT raise three interesting questions.

First, why do iNKT cells accumulate in AT? The abundance of lipid antigens, together with the lipid APC function of CD1d-proficient adipocytes, may contribute importantly to this phenomenon. In mouse and human liver, lipid processing and high CD1d expression by various cell types also create an iNKT niche (48, 49). Moreover, the enrichment of CCR2$^+$ iNKT cells in human

AT suggests chemotaxis by AT-secreted MCP-1, reminiscent of AT-resident macrophages (50). The plethora of AT-secreted factors (43) may well include additional molecules affecting chemotaxis, proliferation, and function of AT-resident iNKT cells.

Second, are liver or muscle, as important regulators of glucose tolerance along with AT, involved in the insulin resistance observed in CD1d-null mice? LFD-fed CD1d-null mice showed none of the pathological alterations associated with liver-mediated insulin resistance. A primary role for muscle tissue, another key regulator of whole-body insulin sensitivity, also seems unlikely, as iNKT cell numbers in muscle appear to be low (51). Nevertheless, we cannot exclude secondary roles for the liver and muscle in the insulin resistance following CD1d deficiency. As in obesity, the adipocyte dysfunction in the LFD-fed CD1d-null mice, characterized by adipocyte hypertrophy and altered adipokine secretion, may well affect the insulin sensitivity of secondary tissues such as liver and muscle (1, 43). We have thereby come to the third question.

What function do iNKT cells exert in AT? Our results indicate that iNKT cells should be included in the list of AT-resident immune cells mediating glucose tolerance: AT-resident macrophages (15, 16), T cells (9, 13, 14), B cells (52), eosinophils (10), and mast cells (53). AT-resident iNKT cells appear to be unique, though, in their communication with adipocytes. The expression of functional CD1d in adipocytes and modulation of iNKT cell function fuel the hypothesis that adipocytes, via lipid presentation to iNKT cells, exert control over the local immune response in AT (24). Similar to other tissues (54), iNKT cells may exert immunoregulatory roles in concert with AT-resident Tregs. Indeed, the increased Treg numbers in AT upon depletion or knockdown of iNKT cells suggest partial compensation of the iNKT loss by Tregs. Accordingly, depletion of AT-resident Tregs in CD1d-null mice on a LFD aggravated the already existing insulin resistance. The adipocyte dysfunction in CD1d-null mice observed here, however, also fuels an alternative hypothesis. Along with indirectly affecting adipocyte function via immune modulation, iNKT cells may also directly control adipocyte function: the iNKT cytokine IL-4, secreted at high levels by AT-resident compared with spleen-derived iNKT cells, is known to improve insulin sensitivity via STAT6 activation (55). IL-13, which is also produced by AT-resident iNKT cells under basal conditions, may also affect adipocyte function, but this area has not been explored so far. Interestingly, we found that AT-resident iNKT cells are also capable of producing IFN-γ when stimulated with αGalCer. As IFN-γ has been associated with insulin resistance in cultured adipocytes (56, 57) and in vivo (14, 58), these findings suggest that, in contrast to the protective role we observed under LFD conditions, iNKT cells could contribute to the development of insulin resistance under other conditions. Indeed, some recent reports indicate that depletion of iNKT cells can improve insulin sensitivity under HFD conditions (59–61). The exact role of iNKT cells under HFD conditions is, however, unclear, as other studies, and the present study, failed to detect a prominent effect of iNKT cell depletion on glucose homeostasis (26–28). Of note, the decreased number of AT-resident iNKT cells in obese human individuals and in mice under long-term HFD conditions may explain the marginal effects of iNKT cell depletion under HFD conditions (refs. 25, 26, and the present study). Future studies are required to establish the exact roles of iNKT-produced cytokines in mediating adipocyte (dys)function and insulin resistance under HFD conditions.

Finally, iNKT cells are known to bridge innate and adaptive immunity, as they can rapidly release high doses of immune polarizing cytokines upon lipid/CD1d complex binding (17–19). Upon prolonged stimulation, iNKT cell numbers are known to decrease and iNKT cells become anergic (62). This physiological role of iNKT cells, together with the insulin-resistant phenotype of CD1d-null iNKT cell–deficient mice under LFD conditions, supports a key role for AT-resident iNKT cells as a first line of defense against adipocyte dysfunction, AT inflammation, and insulin resistance. Importantly, AT-resident iNKT cell function seems to depend on diet composition, duration of the diet, and possibly also indigenous gut microbiota (63). The protective role of iNKT cells appears most explicit under long-term LFD conditions, as Kotas et al. recently failed to observe a protective role of iNKT cells under normal chow conditions in 7- to 10-week-old mice (28). The anti-inflammatory phenotype of AT-resident iNKT cells we observed under unstimulated conditions, with high IL-4 and IL-13 production, together with the strong upregulation of IFN-γ production upon stimulation with the exogenous lipid antigen αGalCer, fuels the hypothesis that AT-resident iNKT cell function is determined by dietary factors, possibly in combination with AT lipid autoantigens. The capacity of adipocytes to modulate iNKT cell function in a CD1d-mediated fashion offers a tempting adipocyte-centered perspective on the mechanisms behind iNKT cell activation. CD1d-dependent adipocyte–iNKT cell interactions may play a key role in the maintenance of healthy AT under LFD conditions.

Methods

Animal studies. WT C57BL/6J mice (8 weeks; Charles River), CD1d-null mice (30), and Jα18-null mice (31) that had been backcrossed to C57BL/6J for 10–12 generations were age matched and fed standard chow until age 10–11 weeks and subsequently fed a LFD (10 kcal% fat; Research Diets, D12450B) or HFD (45 kcal% fat; Research Diets, D12451) for 18–19 weeks. For the IP-GTT, mice (age 28 weeks) were fasted overnight, glucose was injected intraperitoneally (0.5 g/kg body weight), and blood glucose levels were measured before and at multiple time points after glucose injection (Accu-chek, Roche). Plasma was frozen at multiple time points for insulin measurements. For the iNKT cell and Treg depletion studies (Figure 1, J and K, Figure 3, F and G, Supplemental Figure 1A, and Supplemental Figure 3C), WT C57BL/6J mice (8 weeks; Charles River) were fed standard chow until age 10 weeks and subsequently fed LFD for 6 weeks. In the fifth week of LFD feeding, weight-matched groups received 3 intraperitoneal injections of 300 μg αNK1.1 antibody (clone PK136), 3 injections of 250 μg αCD25 antibody (clone PC61), or isotype antibody injections, in agreement with established iNKT and Treg depletion models (32, 64). (Note that the αNK1.1 antibody also depletes NK cells.) In the sixth week of LFD feeding, all mice underwent an IP-GTT (1 g/kg body weight glucose) before sacrifice. For the in vivo challenge with αGalCer, WT C57BL/6J mice (10 weeks) fed LFD for 18 weeks were injected intraperitoneally with either vehicle (PBS; $n = 10$) or αGalCer ($n = 10$) and underwent an IP-GTT (1 g/kg body weight glucose) 3 days afterward. For DEXA, fat mass was measured by DEXA scan under general anesthesia (isoflurane/N_2O/O_2) using a PIXImus imager (GE Lunar).

Isolation of mouse leukocytes and flow cytometry. Murine visceral (epididymal) and subcutaneous AT was collected, washed in PBS, and digested for 45 minutes with collagenase type II (Sigma-Aldrich) and DNAse I (Roche). Stromal vascular cells (SVCs) were pelleted by centrifugation, incubated for 20 minutes with NH_4Cl erythrocyte lysis buffer, and passed through a 100-μm cup filter (BD). Simultaneously, spleens were minced through a 70-μm mesh filter (BD) and collected in NH_4Cl lysis buffer. Subsequently,

AT SVCs and spleen cells were washed in FACS buffer (2% fetal calf serum and 0.1% NaN_3 in PBS); preincubated with 10% rat serum in FACS buffer; and stained with mAbs specific for TCRβ, NK1.1, CD3, CD8, CD4, CD25, and a CD1d tetramer (NIH) for lymphocyte phenotyping (for some samples, this was followed by intranuclear staining of Foxp3) or stained with mAbs for CD206, F4/80, TCRβ, a CD1d tetramer (NIH), CD150, and CD11c for macrophage phenotyping. Cells were analyzed by flow cytometry with a FacsCanto II (BD) flow cytometer and FACSDiva (BD) and FlowJo (Tree Star Inc.) software.

αGalCer stimulation of iNKT cells for intracellular staining. WT C57BL/6J mice (10 weeks) received an intraperitoneal injection of either 5 μg αGalCer (n = 4) or vehicle (n = 4). The next day, the mice were sacrificed, and AT SVCs and spleen cells were extracted and dissolved in RPMI medium containing 10% fetal calf serum, 1% penicillin/streptomycin, and 0.1% GolgiPlug (BD) for 2 hours. Subsequently, after preincubation with 10% rat serum in FACS buffer, cells were stained with mAbs for TCRβ, NK1.1, and a CD1d tetramer (NIH) to identify the iNKT cells, followed by intracellular staining for IL-4 (BD), IFN-γ (BD), IL-13 (BioLegend), and the corresponding isotype antibodies to determine intracellular iNKT cytokine levels.

Ex vivo stimulation and intracellular cytokine staining of AT-resident iNKT cells. Extracted AT SVCs and spleen cells of WT C57Bl/6J mice (9 weeks, n = 4) were dissolved in RPMI medium including 10% fetal calf serum and 1% penicillin/streptomycin, and incubated with 5 ng/ml PMA, 1 μg/ml ionomycin, and 0.1% GolgiStop (BD) for 4 hours. Subsequently, intracellular cytokine levels were measured as described above for the αGalCer stimulation.

RNA extraction, quantitative PCR, and microarray analysis. Snap-frozen epididymal AT was homogenized and RNA was extracted using TRIzol (Invitrogen). RNA was purified on an RNeasy Micro column (QIAGEN), RNA integrity was checked with a Bioanalyzer (Agilent), and cDNA synthesis was performed with iScript (Bio-Rad). Quantitative PCR with SYBR Green (Bio-Rad) was run on a MyiQ machine (Bio-Rad). Primers for quantitative RT-PCR were designed with the universal probe library (Roche) and are described in Supplemental Table 1. Microarray experiments were performed as described before (65). RNA samples from 4–6 mice per experimental group were used for microarray analysis. One hundred nanograms of RNA per sample was hybridized to an Affymetrix GeneChip Mouse Gene 1.1 ST 24 array plate according to the manufacturer's instructions. Arrays were normalized with the robust multiarray average (RMA) method (66, 67). Probe sets were defined according to Dai et al. (68) with CDF version 13.0.2 based on Entrez identifiers. The probes present on these arrays target 21,212 unique genes. Genes were only taken into account if the intensity value was greater than 20 on at least 3 arrays and the interquartile range of the intensity values was greater than 0.1 (log_2) across the experiment. These criteria were met by 14,444 genes. Microarray data have been submitted to the Gene Expression Omnibus database (GEO number GSE39534).

Mouse plasma measurements. Mouse EDTA plasma was harvested after centrifugation and stored at –80°C until analysis. Mouse plasma adipokines were measured with Milliplex mouse adipokine kits (Millipore), according to the manufacturer's instructions. Measurements and data analysis were performed on a Bio-Plex system in combination with Bio-Plex manager software version 4.1.1 (Bio-Rad). AST and ALT levels in mouse EDTA plasma were measured at the diagnostic laboratory of the University Medical Centre Utrecht with a Beckman Coulter DxC chemistry analyzer.

Plasma lipoproteins were separated using fast protein liquid chromatography (FPLC). Pooled plasma (0.2 ml) was injected into a Superose 6B 10/300 column (GE Healthcare Life Sciences) and eluted at a constant flow of 0.5 ml/min with PBS (pH 7.4). The effluent was collected in 0.5-ml fractions and FFA, triglyceride, and cholesterol levels were determined (Instruchemie). Plasma glycerol was measured with a commercially available kit from Instruchemie.

Adipocyte morphometry, AT and liver immunohistochemistry, and liver triglycerides. Morphometry of individual adipocytes was performed as described (69). H&E staining of AT and liver sections was performed using standard protocols. Oil red O (ORO) stock solution was prepared by dissolving 0.5 g ORO (Sigma-Aldrich, O-0625) in 100 ml isopropanol. ORO working solution was prepared by mixing 30 ml ORO stock with 20 ml dH_2O, followed by filtration. Sections (5 μm) were cut from frozen liver sections embedded in O.C.T. Sections were air dried for 30 minutes, followed by fixation in 4% formaldehyde for 10 minutes (4% formaldehyde). Sections were immersed in ORO working solution for 15 minutes, followed by 2 rinses with dH_2O. Hematoxylin staining of nuclei was subsequently carried out for 5 minutes, followed by several rinses with dH_2O. Sections were mounted in aqueous mountant (Imsol).

Liver triglycerides were determined in liver homogenates prepared in buffer containing 250 mM sucrose, 1 mM EDTA, and 10 mM Tris-HCl at pH 7.5 using a commercially available kit (Instruchemie) according to the manufacturer's instructions.

Human subjects. Human abdominal subcutaneous AT samples and blood (sodium heparin) were obtained from 6 healthy female donors during elective abdominoplastic surgery in Bergman Beauty Clinics, Bilthoven, the Netherlands. Immune cell isolations were performed immediately after surgery.

Isolation of human lymphocytes and flow cytometry. SCAT was collected and finely minced, washed in DPBS (Invitrogen), and digested with collagenase type II (Sigma-Aldrich) and DNAse I (Roche). SVCs were filtered over a 100-μm cup filter (BD) and pelleted by centrifugation. After NH_4Cl erythrocyte lysis, SVCs were filtered over a 50-μm cup filter (BD) and pelleted by centrifugation. Simultaneously, PBMCs were isolated from the patients' blood as described previously (70). SVCs and PBMCs were washed in FACS buffer, preincubated with 10% mouse serum in FACS buffer, and stained with mAbs specific for Vα24, Vβ11, CD3, CD4, CD8, CD56, CD95, and a CD1d tetramer (NIH). Furthermore, adhesion factor and chemokine receptor expression was studied with mAbs specific for CD62L, CD11b, CCR2, CCR4, CCR5, CCR7, CXCR2, CXCR3, CXCR6, and CX3CR1. Cells were analyzed by flow cytometry as described above.

Human adipocytes, lentiviral overexpression, and knockdown of human CD1d. The human preadipocyte SGBS cell line was cultured and differentiated into adipocytes as described previously (46, 71). Full-length cDNA encoding human CD1d was cloned into a pLenti CMV vector (Addgene). The shRNA construct for human CD1d was provided in a pLKO.1 vector (Sigma-Aldrich, clone NM_001766.2-814s1c1). Lentiviral particles were produced in 293T cells. After lentiviral infection, SGBS preadipocytes were kept on 2 μg/ml puromycin. Stably transduced cells were used for the adipocyte–iNKT cell interaction studies.

The adiponectin secretion of SGBS adipocytes transduced with empty vector and CD1d shRNA constructs was measured making use of a recently developed and validated multiplex immunoassay (72).

(Pre)adipocyte–iNKT cell interaction study. Untransduced, CD1d shRNA–transduced, and CD1d-overexpressing human SGBS (pre)adipocytes were incubated with αGalCer for 24 hours and with and without CD1d blocking antibody (1 μg/ml CD1d mAb clone 51.1, BioLegend) for 1 hour. Subsequently, iNKT cell lines (>70% CD1d-restricted iNKT cells) from 5 different blood donors, generated as described previously (47), were incubated with the preadipocytes and adipocytes for 18 hours in RPMI medium (Invitrogen) supplemented with 10% human AB^+ serum, 100 μg penicillin/ml, and 100 μg streptomycin/ml (Invitrogen) and IL-2 (10 U/ml). For the last 6 hours, media were supplemented with 0.1% GolgiStop (BD). Finally, the suspended iNKT cell fraction was pelleted for intracellular cytokine staining, and the supernatant was stored at –80°C until analysis of cytokine levels. Cytokine levels were measured with a cytokine multiplex immunoassay, as described recently (72).

Statistics. Data are presented as mean ± SEM, unless otherwise indicated. Statistical significance between 2 groups was determined using 2-tailed Student's *t* tests for normally distributed data and Mann-Whitney *U* tests for nonparametric analyses. *P* values less than 0.05 were considered significant.

Study approval. All mouse study protocols were approved by the Utrecht University Ethical Committee for Animal Experimentation (protocol 2010.III.07.083 and 2011.III.06.061) and were in accordance with Dutch laws on animal experimentation. The study protocol for collection of human samples was approved by the local medical Ethical Committee of the University Medical Center Utrecht (protocol 10-159/C), and oral and written consent was obtained.

Acknowledgments

The authors thank members of the Prakken, Boes, and Kalkhoven laboratories for helpful discussions and the NIH Tetramer Facility for providing the CD1d tetramers. We also thank A. Ostroveanu, S. Versteeg, A. van der Sar, R. Wichers, I. Tasdelen (University Medical Cent Utrecht), and W. Dijk (Wageningen University, Wageningen, the Netherlands.) for technical assistance; M.V. Boekschoten (Wageningen University) for help in analyzing the microarray data; and L. Meij and C. Resius (Bergman Beauty Clinics, Bilthoven, the Netherlands) for assistance with patient recruitment. We thank A. Oosting (Danone, Wageningen) for assistance with DEXA. This study was supported by the research program of The Netherlands Metabolomics Centre, which is part of The Netherlands Genomics Initiative (NGI)/Netherlands Organization for Scientific Research (NWO), and by the Dutch Technology Foundation (STW), which is the applied science division of NWO, and the Technology Programme of the Ministry of Economic affairs.

Received for publication January 5, 2012, and accepted in revised form July 5, 2012.

Address correspondence to: Marianne Boes, Department of Pediatric Immunology, University Medical Centre Utrecht, Wilhelmina Children's Hospital, Lundlaan 6, Post box 85090, KC.01.069.0, 3584 EA Utrecht, Netherlands. Phone: 31.0.88.75.53328; Fax: 31.0.88.75.55350; E-mail: M.L.Boes@umcutrecht.nl. Or to: Eric Kalkhoven, Department of Metabolic Diseases, University Medical Centre Utrecht, Universiteitsweg 100, Post box 85090, STR3.125, 3584 CG Utrecht, Netherlands. Phone: 31.0.88.75.54258; Fax: 31.0.88.75.68101; E-mail: E.Kalkhoven@umcutrecht.nl.

1. Guilherme A, Virbasius JV, Puri V, Czech MP. Adipocyte dysfunctions linking obesity to insulin resistance and type 2 diabetes. *Nat Rev Mol Cell Biol*. 2008;9(5):367–377.
2. Pickup JC. Inflammation and activated innate immunity in the pathogenesis of type 2 diabetes. *Diabetes Care*. 2004;27(3):813–823.
3. Fernandez-Real JM, Pickup JC. Innate immunity, insulin resistance and type 2 diabetes. *Trends Endocrinol Metab*. 2008;19(1):10–16.
4. Hotamisligil GS. Endoplasmic reticulum stress and the inflammatory basis of metabolic disease. *Cell*. 2010;140(6):900–917.
5. Horng T, Hotamisligil GS. Linking the inflammasome to obesity-related disease. *Nat Med*. 2011; 17(2):164–165.
6. Powell K. Obesity: the two faces of fat. *Nature*. 2007;447(7144):525–527.
7. Eckel RH, Grundy SM, Zimmet PZ. The metabolic syndrome. *Lancet*. 2005;365(9468):1415–1428.
8. Donath MY, Shoelson SE. Type 2 diabetes as an inflammatory disease. *Nat Rev Immunol*. 2011; 11(2):98–107.
9. Feuerer M, et al. Lean, but not obese, fat is enriched for a unique population of regulatory T cells that affect metabolic parameters. *Nat Med*. 2009;15(8):930–939.
10. Wu D, et al. Eosinophils sustain adipose alternatively activated macrophages associated with glucose homeostasis. *Science*. 2011;332(6026):243–247.
11. Ilan Y, et al. Induction of regulatory T cells decreases adipose inflammation and alleviates insulin resistance in ob/ob mice. *Proc Natl Acad Sci U S A*. 2010; 107(21):9765–9770.
12. Lumeng CN, Bodzin JL, Saltiel AR. Obesity induces a phenotypic switch in adipose tissue macrophage polarization. *J Clin Invest*. 2007;117(1):175–184.
13. Nishimura S, et al. CD8+ effector T cells contribute to macrophage recruitment and adipose tissue inflammation in obesity. *Nat Med*. 2009;15(8):914–920.
14. Winer S, et al. Normalization of obesity-associated insulin resistance through immunotherapy. *Nat Med*. 2009;15(8):921–929.
15. Xu H, et al. Chronic inflammation in fat plays a crucial role in the development of obesity-related insulin resistance. *J Clin Invest*. 2003;112(12):1821–1830.
16. Weisberg SP, McCann D, Desai M, Rosenbaum M, Leibel RL, Ferrante AW. Obesity is associated with macrophage accumulation in adipose tissue. *J Clin Invest*. 2003;112(12):1796–1808.
17. Kronenberg M. Toward an understanding of NKT cell biology: progress and paradoxes. *Annu Rev Immunol*. 2005;23:877–900.
18. Godfrey DI, Stankovic S, Baxter AG. Raising the NKT cell family. *Nat Immunol*. 2010;11(3):197–206.
19. Bendelac A, Savage PB, Teyton L. The biology of NKT cells. *Annu Rev Immunol*. 2007;25:297–336.
20. Hammond KJ, Poulton LD, Palmisano LJ, Silveira PA, Godfrey DI, Baxter AG. alpha/beta-T cell receptor (TCR)+CD4-CD8- (NKT) thymocytes prevent insulin-dependent diabetes mellitus in nonobese diabetic (NOD)/Lt mice by the influence of interleukin (IL)-4 and/or IL-10. *J Exp Med*. 1998; 187(7):1047–1056.
21. Hong S, et al. The natural killer T-cell ligand alpha-galactosylceramide prevents autoimmune diabetes in non-obese diabetic mice. *Nat Med*. 2001; 7(9):1052–1056.
22. Sharif S, et al. Activation of natural killer T cells by alpha-galactosylceramide treatment prevents the onset and recurrence of autoimmune Type 1 diabetes. *Nat Med*. 2001;7(9):1057–1062.
23. Lee PT, Putnam A, Benlagha K, Teyton L, Gottlieb PA, Bendelac A. Testing the NKT cell hypothesis of human IDDM pathogenesis. *J Clin Invest*. 2002;110(6):793–800.
24. Matzinger P, Kamala T. Tissue-based class control: the other side of tolerance. *Nat Rev Immunol*. 2011; 11(3):221–230.
25. Lynch L, O'Shea D, Winter DC, Geoghegan J, Doherty DG, O'Farrelly C. Invariant NKT cells and CD1d(+) cells amass in human omentum and are depleted in patients with cancer and obesity. *Eur J Immunol*. 2009;39(7):1893–1901.
26. Ji Y, et al. Activation of natural killer T cells promotes M2 Macrophage polarization in adipose tissue and improves systemic glucose tolerance via interleukin-4 (IL-4)/STAT6 protein signaling axis in obesity. *J Biol Chem*. 2012;287(17):13561–13571.
27. Mantell BS, Stefanovic-Racic M, Yang X, Dedousis N, Sipula IJ, O'Doherty RM. Mice lacking NKT cells but with a complete complement of CD8+ T-cells are not protected against the metabolic abnormalities of diet-induced obesity. *PLoS One*. 2011;6(6):e19831.
28. Kotas ME, et al. Impact of CD1d deficiency on metabolism. *PLoS One*. 2011;6(9):e25478.
29. West DB, York B. Dietary fat, genetic predisposition, and obesity: lessons from animal models. *Am J Clin Nutr*. 1998;67(3 suppl):505S–512S.
30. Exley MA, et al. CD1d-reactive T-cell activation leads to amelioration of disease caused by diabetogenic encephalomyocarditis virus. *J Leukoc Biol*. 2001; 69(5):713–718.
31. Cui J, et al. Requirement for Valpha14 NKT cells in IL-12-mediated rejection of tumors. *Science*. 1997;278(5343):1623–1626.
32. Lappas CM, Day YJ, Marshall MA, Engelhard VH, Linden J. Adenosine A2A receptor activation reduces hepatic ischemia reperfusion injury by inhibiting CD1d-dependent NKT cell activation. *J Exp Med*. 2006;203(12):2639–2648.
33. Wang M, Ellison CA, Gartner JG, HayGlass KT. Natural killer cell depletion fails to influence initial CD4 T cell commitment in vivo in exogenous antigen-stimulated cytokine and antibody responses. *J Immunol*. 1998;160(3):1098–1105.
34. Saltiel AR. New perspectives into the molecular pathogenesis and treatment of type 2 diabetes. *Cell*. 2001;104(4):517–529.
35. Marchesini G, et al. Nonalcoholic fatty liver, steatohepatitis, and the metabolic syndrome. *Hepatology*. 2003;37(4):917–923.
36. Schwartzberg PL, Mueller KL, Qi H, Cannons JL. SLAM receptors and SAP influence lymphocyte interactions, development and function. *Nat Rev Immunol*. 2009;9(1):39–46.
37. Baev DV, et al. Impaired SLAM-SLAM homotypic interaction between invariant NKT cells and dendritic cells affects differentiation of IL-4/IL-10-secreting NKT2 cells in nonobese diabetic mice. *J Immunol*. 2008;181(2):869–877.
38. Lumeng CN, DelProposto JB, Westcott DJ, Saltiel AR. Phenotypic switching of adipose tissue macrophages with obesity is generated by spatiotemporal differences in macrophage subtypes. *Diabetes*. 2008;57(12):3239–3246.
39. Stienstra R, Mandard S, Patsouris D, Maass C, Kersten S, Muller M. Peroxisome proliferator-activated receptor alpha protects against obesity-induced hepatic inflammation. *Endocrinology*. 2007;148(6):2753–2763.
40. Duval C, et al. Adipose tissue dysfunction signals progression of hepatic steatosis towards nonalcoholic steatohepatitis in C57BL/6 mice. *Diabetes*. 2010;59(12):3181–3191.
41. Shoelson SE, Lee J, Goldfine AB. Inflammation and insulin resistance. *J Clin Invest*. 2006; 116(7):1793–1801.
42. Phan J, Reue K. Lipin, a lipodystrophy and obesity gene. *Cell Metab*. 2005;1(1):73–83.
43. Ouchi N, Parker JL, Lugus JJ, Walsh K. Adipokines in inflammation and metabolic disease. *Nat Rev*

Immunol. 2011;11(2):85–97.
44. Kim CH, Johnston B, Butcher EC. Trafficking machinery of NKT cells: shared and differential chemokine receptor expression among V alpha 24(+)V beta 11(+) NKT cell subsets with distinct cytokine-producing capacity. *Blood*. 2002;100(1):11–16.
45. Sell H, Eckel J. Monocyte chemotactic protein-1 and its role in insulin resistance. *Curr Opin Lipidol*. 2007;18(3):258–262.
46. Fischer-Posovszky P, Newell FS, Wabitsch M, Tornqvist HE. Human SGBS cells – a unique tool for studies of human fat cell biology. *Obes Facts*. 2008;1(4):184–189.
47. Exley MA, Wilson B, Balk SP. Isolation and functional use of human NKT cells. *Curr Protoc Immunol*. 2010;Chapter 14:Unit 14.11.
48. Sprengers D, et al. Critical role for CD1d-restricted invariant NKT cells in stimulating intrahepatic CD8 T-cell responses to liver antigen. *Gastroenterology*. 2008;134(7):2132–2143.
49. Takeda K, Hayakawa Y, Van Kaer L, Matsuda H, Yagita H, Okumura K. Critical contribution of liver natural killer T cells to a murine model of hepatitis. *Proc Natl Acad Sci U S A*. 2000;97(10):5498–5503.
50. Kanda H, et al. MCP-1 contributes to macrophage infiltration into adipose tissue, insulin resistance, and hepatic steatosis in obesity. *J Clin Invest*. 2006; 116(6):1494–1505.
51. Vetrone SA, et al. Osteopontin promotes fibrosis in dystrophic mouse muscle by modulating immune cell subsets and intramuscular TGF-beta. *J Clin Invest*. 2009;119(6):1583–1594.
52. Winer DA, et al. B cells promote insulin resistance through modulation of T cells and production of pathogenic IgG antibodies. *Nat Med*. 2011; 17(5):610–617.
53. Liu J, et al. Genetic deficiency and pharmacological stabilization of mast cells reduce diet-induced obesity and diabetes in mice. *Nat Med*. 2009;15(8):940–945.
54. La Cava A, Van Kaer L, Fu Dong S. CD4+CD25+ Tregs and NKT cells: regulators regulating regulators. *Trends Immunol*. 2006;27(7):322–327.
55. Ricardo-Gonzalez RR, et al. IL-4/STAT6 immune axis regulates peripheral nutrient metabolism and insulin sensitivity. *Proc Natl Acad Sci U S A*. 2010; 107(52):22617–22622.
56. Wada T, et al. Both type I and II IFN induce insulin resistance by inducing different isoforms of SOCS expression in 3T3-L1 adipocytes. *Am J Physiol Endocrinol Metab*. 2011;300(6):E1112–E1123.
57. McGillicuddy FC, et al. Interferon gamma attenuates insulin signaling, lipid storage, and differentiation in human adipocytes via activation of the JAK/STAT pathway. *J Biol Chem*. 2009;284(46):31936–31944.
58. O'Rourke RW, et al. Systemic inflammation and insulin sensitivity in obese IFN-gamma knockout mice. *Metabolism*. 2012;61(8):1152–1161.
59. Ohmura K, et al. Natural killer T cells are involved in adipose tissues inflammation and glucose intolerance in diet-induced obese mice. *Arterioscler Thromb Vasc Biol*. 2010;30(2):193–199.
60. Satoh M, et al. Type II NKT cells stimulate diet-induced obesity by mediating adipose tissue inflammation, steatohepatitis and insulin resistance. *PloS One*. 2012;7(2):e30568.
61. Wu L, et al. Activation of invariant natural killer T cells by lipid excess promotes tissue inflammation, insulin resistance, and hepatic steatosis in obese mice. *Proc Natl Acad Sci U S A*. 2012;109(19):E1143–E1152.
62. Van Kaer L, Parekh VV, Wu L. Invariant natural killer T cells: bridging innate and adaptive immunity. *Cell Tissue Res*. 2011;343(1):43–55.
63. Cani PD, Delzenne NM. Interplay between obesity and associated metabolic disorders: new insights into the gut microbiota. *Curr Opin Pharmacol*. 2009;9(6):737–743.
64. Wheeler K, et al. Regulatory T cells control tolerogenic versus autoimmune response to sperm in vasectomy. *Proc Natl Acad Sci U S A*. 2011;108(18):7511–7516.
65. Lichtenstein L, et al. Angptl4 protects against severe proinflammatory effects of saturated fat by inhibiting fatty acid uptake into mesenteric lymph node macrophages. *Cell Metab*. 2010;12(6):580–592.
66. Bolstad BM, Irizarry RA, Astrand M, Speed TP. A comparison of normalization methods for high density oligonucleotide array data based on variance and bias. *Bioinformatics*. 2003;19(2):185–193.
67. Irizarry RA, Bolstad BM, Collin F, Cope LM, Hobbs B, Speed TP. Summaries of Affymetrix GeneChip probe level data. *Nucleic Acids Res*. 2003;31(4):e15.
68. Dai M, et al. Evolving gene/transcript definitions significantly alter the interpretation of GeneChip data. *Nucleic Acids Res*. 2005;33(20):e175.
69. Stienstra R, Duval C, Keshtkar S, van der Laak J, Kersten S, Muller M. Peroxisome proliferator-activated receptor gamma activation promotes infiltration of alternatively activated macrophages into adipose tissue. *J Biol Chem*. 2008;283(33):22620–22627.
70. van de Ven AA, et al. Lymphocyte characteristics in children with common variable immunodeficiency. *Clin Immunol*. 2010;135(1):63–71.
71. Jeninga EH, et al. Peroxisome proliferator-activated receptor gamma regulates expression of the anti-lipolytic G-protein-coupled receptor 81 (GPR81/Gpr81). *J Biol Chem*. 2009;284(39):26385–26393.
72. Schipper HS, et al. A multiplex immunoassay for human adipokine profiling. *Clin Chem*. 2010; 56(8):1320–1328.